A COMPARISON BETWEEN CRISM AND CHEMCAM PASSIVE SKY WATER VAPOR RETRIEVALS OVER GALE CRATER

A. SJ. Khayat[1,2] *(alain.khayat@nasa.gov)*, **McConnochie**[1,3], **T.**, and **M. D. Smith**[1]. [1]*NASA Goddard Space Flight Center, Greenbelt, MD, USA,*[2]*Center for Research and Exploration in Space Science & Technology (CRESST II), Department of Astronomy, University of Maryland, MD, USA,*[3]*Space Science Institute, Boulder, CO, USA.*

Background

Spacecraft observations provide a global view of the Martian atmosphere by monitoring its behavior across the planet. In contrast, landers and rovers provide information on the local environment around their landing sites.

The Mars Reconnaissance Orbiter (MRO) has been making observations since November 2006. A key objective of the Compact Reconnaissance Imaging Spectrometer for Mars (CRISM) on MRO (Murchie et al., 2007) is the "*atmospheric monitoring to characterize the spatial and temporal properties of the atmosphere for the studies of climate, weather and photochemistry*". We report atmospheric water vapor column abundances at a spatial resolution of ~ 1 km from observations taken over Gale crater, the landing site of the Mars Science Laboratory (MSL). The 61 targeted mode observations shown in Figure 1 span a little more than 3 Mars years (MY) from MY 28 at L_s = 116° (October 04, 2006) to MY 31 at L_s = 101° (April 24, 2012). The seasonal cycle of water vapor above Gale is compared against that from reprocessed MSL Curiosity rover ChemCam passive sky observations using updated gas absorption parameters and covering the period between MY 31 at L_s = 291° (March 30, 2013) and MY 35 at L_s = 42° (June 20, 2019.

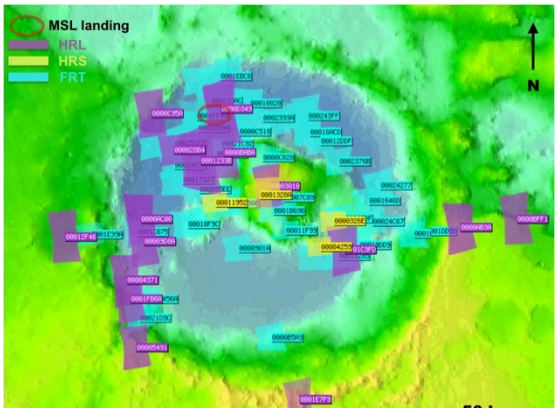

Figure 1: CRISM targeted observations used in this work overlaying a topography map by the Mars Orbiter Laser Altimeter. Most of the observations were taken around the MSL landing site indicated by the red ellipse. The regions covered by the observations are indicated by the shaded areas in purple, yellow and cyan colors for the Half Resolution Long (HRL), Half Resolution Short (HRS) and Full Resolution Targeted (FRT) observations, respectively, and annotated with their numbers.

Methodology

CRISM is affected by the "spectral smile", an artifact caused by the optical distortions onto the instrument's detector, leading to a non-uniform variation of the central wavelength and the point spread function (PSF) of the detector matrix in the across track direction (Ceamanos & Doute, 2010). This effect is minimal around the central columns, commonly referred to as the "sweet spot". Previous water vapor abundance retrievals (e.g., Smith et al., 2009; 2018; Khayat et al., 2019) were conducted by binning the central 100 × 100 pixels, covering a central area 2 km × 2 km in every CRISM image, and others (Khayat et al., 2020) used pixels in the along-track direction to track the changes of water vapor abundance over the polar troughs. We derived the wavelength offset for every pixel in Figure 2 and used it as an input in the radiative transfer code to cover a larger portion of every CRISM observation.

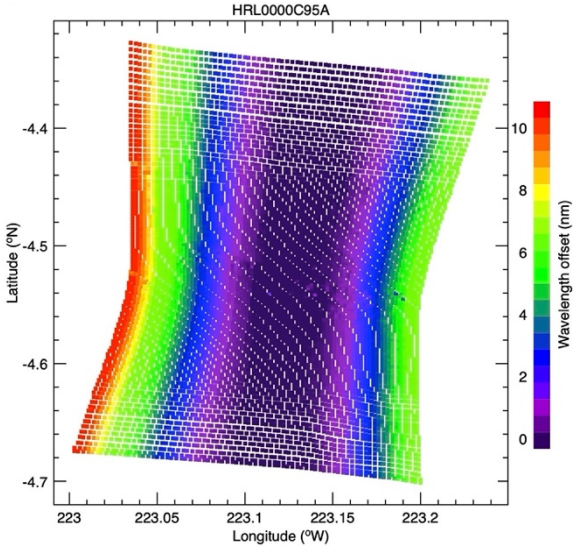

Figure 2: Area on Mars covered by the CRISM observation HRL0000C95A taken on September 19, 2008 at L_s = 129.4°, and centered at longitude 223.12 °W and latitude 4.51°S. The map of the derived wavelength offset shows an increase in offset in the cross-track dimension, but no dependence in the along-track direction.

The retrieval algorithm used here was first described in Smith et al. (2009) and subsequently adapted and used to provide CRISM atmospheric water vapor retrievals over surface ice in the north polar regions (Khayat et al., 2019, 2020), and to

characterize the climatology of carbon monoxide by retrieving the seasonal and spatial variations of the molecule's mixing ratio (Smith et al., 2018; 2021). The water vapor column abundance is retrieved by adjusting the water vapor abundance after correcting for the retrieved wavelength offset at every pixel (see Fig. 2) until the computed spectrum best matches the observed CRISM spectrum.

The retrieval results from ChemCam observations presented in McConnochie et al. (2018) provided total column abundance of water vapor until MY 33 at L_s = 127°. McConnochie reprocessed the data here using updated versions of the line list parameters from the HITRAN 2016 database (Gordon et al., 2017) including parameters for the CO_2 band near 783 nm and 789 nm that is used a reference in the H_2O retrievals and extended the coverage to include two additional Mars years until MY 35 at L_s =42° (June 20, 2019).

Results and conclusion

The seasonal trend of water vapor in Figure 3 as retrieved by CRISM (black diamonds) follows what is expected over equatorial regions with the timing of the aphelion minimum and the maximum around northern autumn at a time when the sublimated water vapor transported from the north polar region reaches equatorial regions (e.g., Smith et al., 2009; McConnochie et al., 2018). At the beginning of northern spring, the scaled water vapor column abundance over Gale shows values around 7 pr-µm, followed by a decline in the water abundance reaching values as low as 3 pr-µm at the driest time of the year over Gale around mid to late of northern spring at L_s = 60°. Later in the season the water vapor column abundance follows a steadily rising trend from 3 pr-µm to peak values ~ 15 pr-µm around the end of northern summer and early northern autumn at L_s = 180°. The water abundance column abundance shows a steady decline during northern autumn and winter, reaching values between 6 pr-µm and 8 pr-µm in the L_s = 315° - 360° period.

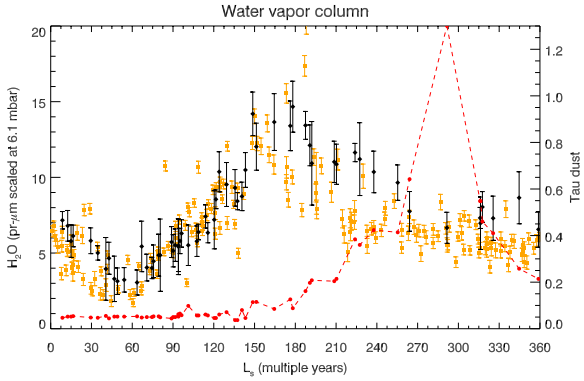

Figure 3: Water vapor column abundance scaled to a surface pressure of 6.1 mbar. The black diamonds indicate the median value over each observation of the retrieved CRISM water vapor column from multiple Mars years between MY 26 at L_s = 116° and MY 31 at L_s = 101° conducted at ~ 15:00 LTST. The error bars indicate the standard deviation over the water columns across every observation. The squares in orange indicate the updated ChemCam water vapor column retrievals for observations taken during multiple Mars years between MY 31 at L_s = 291° and MY 35 at L_s = 42° from 7:15 to 14:24 LTST. The filled red circles represent the seasonal THEMIS dust opacity for each corresponding to the CRISM observations.

As a result of implementing updated spectral parameters, there is modestly more water vapor in the new ChemCam retrievals compared to the results shown in McConnochie et al. (2018). The results in Figure 3 (orange squares) show some variations during northern spring during the L_s = 15 -70° period, with retrieved water vapor abundances between 2.5 pr-µm and 8 pr-µm at L_s = 30°. Other variations in the retrievals are observed between L_s =150° and 270°, with a maximum range of ~10 pr-µm (between ~7 pr-µm and ~17 pr-µm) around L_s =180°.

The annual variation of water vapor from both updated retrievals over multiple Mars years shows a much closer match than before to McConnochie et al. (2018). A moderate difference occurring in some cases could likely be attributed to the interannual variations in water vapor and to the difference in the retrieval approaches between CRISM and ChemCam and in using different spectral bands of water.

References

Ceamanos, X., and Doute, S., 2010. Spectral Smile Correction of CRISM/MRO Hyperspectral Images. IEEE Transactions on Geosc. and Rem. Sens., 48, no. 11, pp. 3951-3959.

Gordon, I.E., et al., 2017. The HITRAN2016 molecular spectroscopic database, JQRST 203, 3-69.

Khayat, A., et al., 2019. Understanding the Water Cycle Above the North Polar Cap on Mars Using MRO CRISM Retrievals of Water Vapor. Icarus, 321: 722 - 735.

Khayat, A. S.J., et al., 2020. Detections of water vapor increase over the north polar troughs on Mars as observed by CRISM. GRL, 47.

McConnochie, T. et al., 2018. Retrieval of water vapor column abundance and aerosol properties from ChemCam passive sky spectroscopy. Icarus, 307, 294-326.

Murchie, S., R. et al., 2007. Compact Reconnaissance Imaging Spectrometer for Mars (CRISM) on Mars Reconnaissance Orbiter (MRO), JGR 112(E11).

Smith, M.D., et al., 2009. Compact Reconnaissance Imaging Spectrometer observations of water vapor and carbon monoxide. JGR 114, E00D03.

Smith, M.D., et al., 2018. The climatology of carbon monoxide and water vapor on Mars as observed by CRISM and modeled by the GEM-Mars general circulation model. Icarus 301,117–131.

Smith, M.D. et al., 2021. The climatology of carbon monoxide on Mars as observed by NOMAD nadir-geometry observations, Icarus, 362.